SERA
Seismology and Earthquake Engineering
Research Infrastructure Alliance for Europe

DELIVERABLE

D23.3 Methodologies for characterizing the forcing terms for the initiation of seismicity

Work package	WP23
Lead	CNRS
Authors	Bernard, CNRS
Reviewers	-
Approval	Management Board
Status	Final
Dissemination level	Public
Delivery deadline	30.04.2019
Submission date	30.04.2019
Intranet path	DOCUMENTS/DELIVERABLES/SERA_D23.3_Forcing_initiation_seismicity

This project has received funding from the European Union's Horizon 2020 research and innovation programme under grant agreement No 730900.

Table of Contents

Summary

Following the description of the Deliverable D23.3, we developed our research on the following targets: mechanical conditions of the activated faults and their seismogenic potential; space-time evolution of seismicity; loading factors (e.g. local creep, local pore pressure diffusion, remote loading, or fault interaction). We focussed on two densely and continuously monitored fault zones, one in the normal fault setting of the rift of Corinth (Greece), characterizing its seismicity over 15 years, the other in the subduction zone of northern Chile, characterizing one year of precursory seismicity before the 2014, Magnitude 8 Iquique earthquake.

For Chile, the analysis of the background (unclustered) seismicity for one year before the mainshock reveals a seismic quiescence in the deepest part of the interplate contact, coincident with the development of families of repeating earthquakes, which migrated upwards, progressively surrounding the area of the future mainshock asperity, and in particular preceding the main foreshock rupture. We interpret this precursory sequence as a primary destabilization of the deep interplate contact with a long term slow slip possibly combined with pore pressure diffusion, followed by the development of transient creeping upwards, closer to the main seismic asperities.

For Corinth, we show that the analysis of the characteristics of multiplet families contributed to constrain the transient or steady mechanical loading of the main faults: Short-lived multiplets, during seismic swarms, reveal the diffusion of pore pressure pulses at the root of the main outcropping faults, sometimes accompanied by transient creep migration. Deeper, long-lasting, rather cyclic multiplets, spanning many years, are interpreted as rather isolated small asperity clusters forced by continuous creep; their location bordering large scale fault surfaces with depleted seismicity reveals the locked and potentially seismogenic character of the latter.

The association of refined multiplet/repeater studies with space-time statistics (including cluster/background separation) thus appears as a very powerfull approach for constraining transient processes in fault systems, whether related to pore pressure or to slow slip, and for detecting larger scale instabilities which may grow up into large earthquakes.

1 Foreshocks, quiescence and slow slip before the 2014 M8 Iquique (Chile) earthquake

The 2014 Iquique, M8 subduction earthquake, in the northern Chilean seismic gap, was preceded by 3 months of intense, shallow foreshock activity (e.g., Ruiz et al. 2014), coupled with Slow Slip Events (SSEs) detected by GPS and tiltmeter (e.g. Schurr et al., 2014; Socquet et al., 2017). This earthquake broke only part of the gap, leaving a potential for a M=8.5 to 9.0 earthquake. The application of the automatic detection and location method Back-Track BB (Poiata et al. 2016, see also the SERA deliverable D23.1), from January 2012 to the mainshock of April 1rst 2014, for the shallow as for the intermediate depth seismicity, allowed us to produce a rich catalogue, complete down to M=2.6 (the CSN catalogue has a magnitude completeness of 4) (Aden-Antoniow, 2018).

We first investigated the statistical space-time properties of this new catalogue in order to detect possible, yet still unreported interactions between transient deformation of the slab at large depths and slow slip on the interplate, as was suggested by Bouchon et al. (2016). We then looked at the location and activity of repeating earthquakes (repeaters), completing the initial database with events extracted by correlation (template matching). Combining the results from both studies led us to better resolve the growing mechanical instability which triggered the 2014 mainshock, as is presented in detail in Aden-Antoniow (2018).

In the first approach, we separated the global catalogue into its poissonian and its clustered components, following the Zaliapin & Ben Zion (2013) method, based on the decay of interevent interactions with delay and distance. We then focussed on the poissonan activity of the background, using a Kolgomorov-Smirnov (KS) test to detect places and time windows of statistically significant non-stationarity. The test was set on a 2D grid (5km) on the subducting plate, and the events were counted on a circle of 60 km radius, taking as reference the first 185 days out of the 473 days of the catalogue. We found that the intermediate depth background seismicity did not show any clear anomaly, which does not support the hypothesis of Bouchon et al. (2016) for a large scale, deep activation of the slab. However, the shallow interface seismicity did show a strong rate decrease, as seen in Figure 1.1.

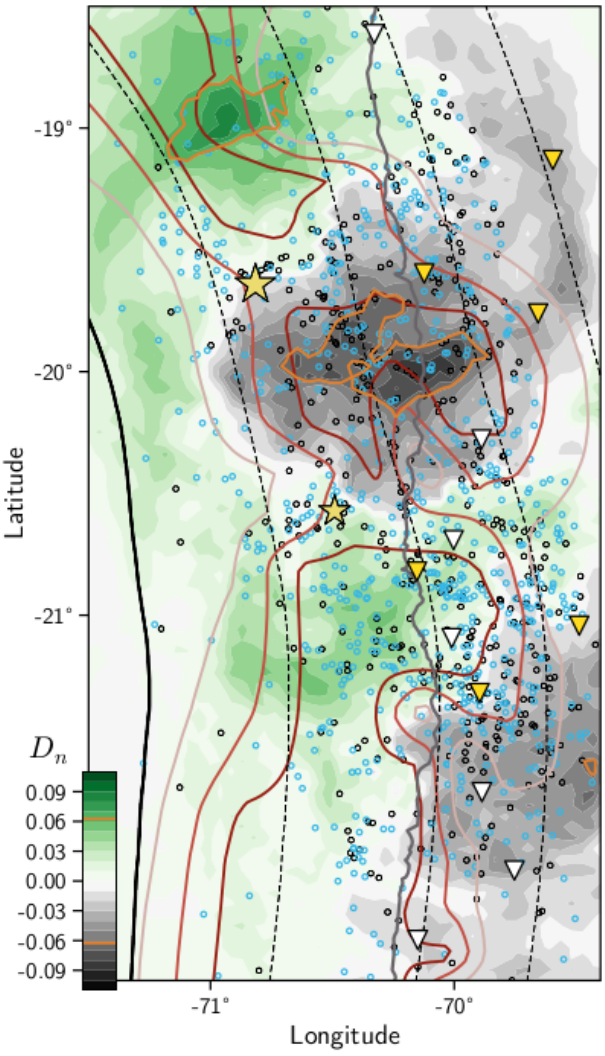

Figure 1.1 – KS estimated spatially for interface background catalogs : December 13 th 2012 - April 1 st 2014. Grey areas are associated to a negative KS criterion Dn which means a lower than expected number of events occurred after the end of reference period. Green (interface background) and Red (intermediate depths background) are regions where a greater than expected number of events occurred after the end of reference period. Orange contour are delimiting areas of negative/positive significance. Black dots mark the seismicity that occurred during the reference period while blue dotes correspond to events which occured after. Red lines are 0.3, 0.6 and 0.9 interseismic coupling coefficient contours (Métois et al. 2016). The solid black line is the trench while dashed black line are isodepth slab-profile every 20km. The two yellow stars are located at the epicenter of the Iquique earthquake (to the north) and its major aftershock. Grey solid line marks the coastline.(Aden-Antoniow, 2018)

Quiescences have been observed many times before large earthquakes (e.g. Wiemer and Wyss 1994, Wu and Chiao 2006, Katsumata 2018). In the present case, if the seismicity decrease concerns interplate earthquakes, it would suggest a local decrease in pore pressure in the subduction channel, related to a pore pressure diffusion outside of this quiescent zone, possibly updip through the subduction channel. Alternatively, if the seismicity decrease concerns the bulk of the mantle wedge, then a slow slip on the interface would explain this quiescence by stress release (stress shadow). Unfortunately, the resolution in the source depths is not accurate enough for distinguishing interplate sources from other events. In both cases, however, one expects a significant stress increase more updip on the interplate contact, through elastic shear or pore pressure transfert. We note that the location of the statistically significant quiescence coincides with the location of the highest interplate coupling in the northern Chili gap, as calculated by Métois et al. (2016), around latitude 20° south, which may provide important clues for setting the stress or friction conditions of this zone.

In the second approach, we focussed on the specific families of repeating earthquakes. We defined a set of well located events in our Back-Track BB catalogue, with sufficient signal-to-noise ratio. We then complemented the family of each event by a « template matching » method, scanning the whole IPOC and the ILN data base for correlated waveforms, from December 13th 2012 to March 31th 2014. This produced 9078 events from 1833 templates (915 from the background seismicity and 918 from the aftershocks, out of which 73% were aftershocks of the March 16th cluster). For each family of repeating earthquakes, we then compute the cumulative coseismic slip, and average their value in 20 km-wide boxes in order to get a smoothed proxy of the aseismic slip on the creeping area around each of them (Figure 1.2).

The resulting image reveals the space-time dynamics of the families of repeaters - and hence of the inferred forcing slow slip -, progressively surrounding the main asperity to be broken during the mainshock. This activation started to the south and to the east (downdip), before the main foreshock of the 16 th of March, after which it developed more updip, consistent with previous studies (Meng et al. 2015, Herman et al. 2016, Kato et al.2016). The location of the most downdip, well developed repeaters appear to coincide with the upper region of the strong quiescence, which is somehow puzzling. A complex coupling process between the deep plate interface and the mantle wedge, and possibly the transient diffusion of pore pressure in or around the interplate contact, as already suggested above, may be considered to explain the simultaneity of background quiescence and localized fault creep. Their relative location is however not accurate enough to propose a more consistent mechanical model, which is probably controlled by unresolved heterogeneities in friction, permeabilities, as well as in stress and pore pressure conditions.

Fluids have been found to take place at the interface in this very particular regions (Yoon et al. 2009; and references therein) and may allow a transition from fast slip to stable slip highlighted by a seismic-quiescence. They have been already introduced as a major parameter controlling the coupling at the interface and modulating the stress in the regions of the Illapel earthquake (Poli et al., 2017) or Maule earthquake (Moreno et al. 2014) , and in northern part of the chilean subduction zone (Pasten-Araya et al. , 2018) . We suggest, with these observations, that fluid circulations along the interplate may have facilitated the reduction of the effective normal stress by the increase of the fluid-pore pressure migration updip, which in turn produced slow slip events around the major asperities.

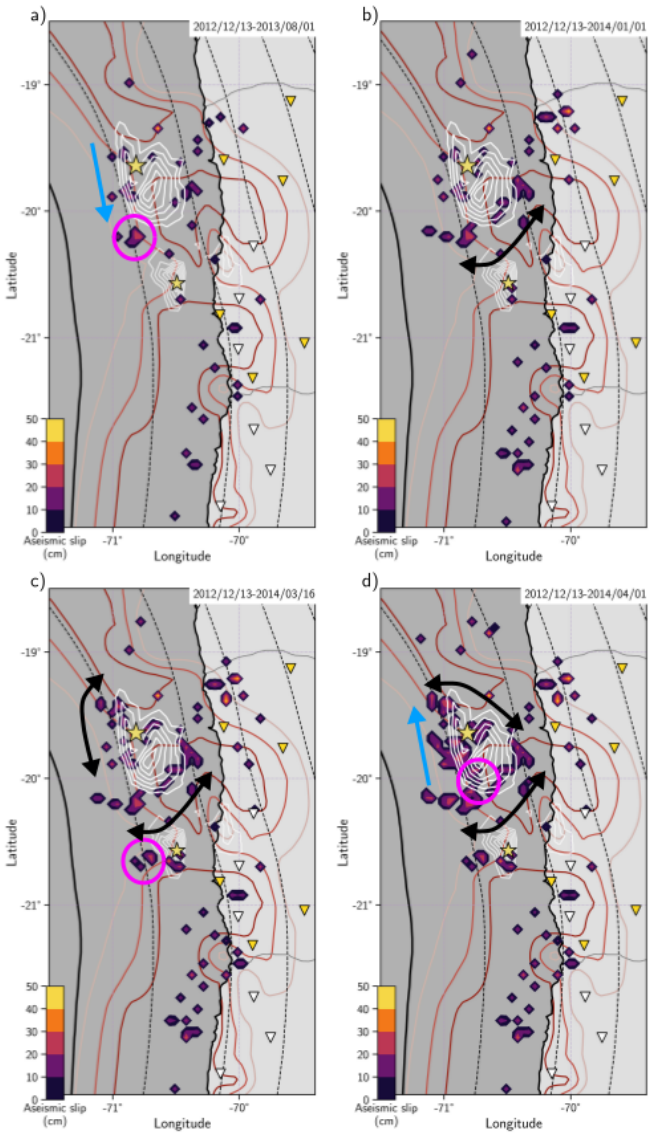

Figure 1.2 – Map of cumulative aseismic slip before the Iquique earthquake : December 2012-April 2014. a), b), c) et d) represent four snapshots, with increasing duration, of the cumulative aseismic slip inferred from repeating earthquakes from dark purple to yellow contours. solid black line : trench ; dashed black line : isodepth contours for every 20km-depth ; red curves for the 0.3, 0.6 and 0.9 interseismic coupling coefficent (Métois et al. 2016). Triangles show the position of the stations used. The white contours delimit the coseismic slip of the Iquique earthquake to the north and its major aftershock represented by yellow stars. ***a. December 2012 - July 2013.*** *The blue arrow reflects the direction of a potential migration of aseismic slip while the purple circle marks the July 2013 cluster.* ***b. December 2012 – December 2013.*** *After July 2013, slip developed southward and in the downdip part of the coseismic slip of the Iquique earthquake .****c. December 2012 – March 16 th 2014.*** *The January 2014 cluster is represented by the purple circle. The aseismic-slip developed anew downdip and to the northwest of the coseismic patch of the mainshock.* ***d. December 2012 – April 1 st 2014.*** *The march cluster is marked by the purple circle while the migration of aseismic slip to the north and the nucleation area of the mainshock is represented by the blue arrow.*

2 Transient creep and pore pressure in the western Corinth Rift

2.1 Seismic and tectonic setting

The western Corinth rift is the target of one of the Near Fault Observatories (NFO) of EPOS, the Corinth Rift Laboratory (CRL, www.crlab.eu). This well developed normal fault system presents the highest microseismicity and strain rate of the euro-mediterranean area, with a rift opening rate of 1.5 cm/year, and several M6-6.5 earthquakes per century. (see e.g., Lambotte et al., 2014) . Here, we analyzed the complete earthquake archive of CRL using both cross-correlations between pairs of event waveforms and accurate differential travel times observed at common stations, in order to identify small-scale fault structures at depth (Duverger et al., 2018). The waveform database was generated by the dense CRL network and includes about 205,000 events between 2000 and 2015. Half of them are accurately

relocated using double-difference techniques (HYPODD). The total relocated seismicity exhibits well-defined clusters at the root of the main normal faults, mainly between 5 and 10 km depth in the middle of the gulf, and illuminates thin active structure planes dipping north about 20° under the northern coast. Some seismicity is still observed in the footwall of the main active faults, along the West and East Helike faults to the South.

We built a multiplet database based on waveform similarity taking into account cross-correlation coefficients weighted by signal-to-noise ratios. This data base can be split into two main sets, short-term and long-term multiplets, well separated by their total duration, larger or smaller than the typical duration of the main swarms (months). The analysis of these two sets led us to improve our understanding of the loading process of the fault system.

2.2 Short-term multiplets, pore pressure, and creep transients

Short-term multiplets are mostly concentrated in the middle of the gulf along the Kamarai fault system, in a 1–2 km thick layer at 6–8 km depth, interpreted as a highly fractured geological layer. They are often associated to slow seismic migration velocities (less than 100 m /day) occurring in this zone during strong swarm episodes, and are thus likely to be triggered by pore pressure variations (Lambotte et al., 2014).

However, we found that the different migration velocities, from 0.05 km/day to several km/day, highlighted in particular during the western 2014 swarms, indicate that both pore pressure and creep diffusion are operating in the fault zone, as the fast migrations (> 1 km/day) observed in the Psathopyrgos fault zone would require unrealistic permeabilities if due to pore pressure, and are more typical of creep diffusion on faults.

Microseismicity migration is illustrated in Figure 2.1. It is interesting to note that the same area at the root of the Psathopyrgos major normal fault, is subject in 2014 first to a slow migration (0.3 km/day), interpreted as pore pressure diffusion, followed 40 days later by a fast migration (3 km/day), interpreted as creep diffusion. The latter is thus possibly favoured by the persistence of a higher pore pressure brought by the first pore pressure episode.

The absence of repeaters among the multiplets belonging to these sequences allows to provide limits to their stressing effects on the nearby locked faults: For each sequence, (1) the increase in pore pressure must be smaller than the average stress drop (typically 1 MPa), and (2), cumulative creep must be smaller than the slip of a single event (typically 1 mm, considering the dominance of magnitude 2 to 2.5). The fact that these multiplets are not reactivated in successive swarms also imposes that the geometry and/or the frictional property of the fracture system in the brittle geological layer is significantly changing in time, most likely through damage and/or fast healing.
The limit of 1 MPa (or less) pore pressure suggests that the activated fault zone stays very close to its failure threshold, steadily loaded by the rift extension. However, it is not clear yet if the pore pressure diffusion is just a passive response to gradients of extensional/compressional strains related to the elastic shear and fault creep due to rift extension, or if the involved fluid provides its own strain energy to the system, thanks to permanent or episodic connection of over-pressurized reservoir in the middle/lower crust.

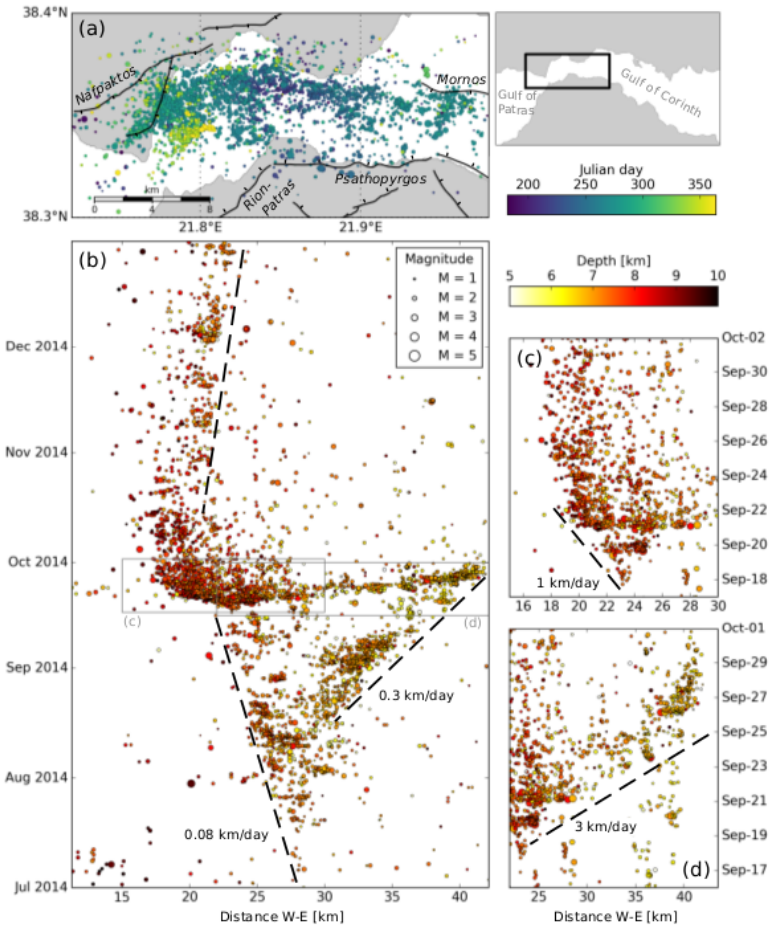

Figure 2.1: Seismicity migration at CRL. Seismic migration velocities during the westernmost swarm in 2014. (a) Map of the seismicity migration along the Psathopyrgos, Nafpaktos and Rion-Patras faults. The longitude 21.6° is 0 km distance. The black lines are the main normal faults. The colorbar represents the time in Julian days of 2014. (b) Temporal evolution of the microseismicity along the longitude. The circle size is proportional to the event magnitude. (c) and (d) are zooms in migrations represented by light gray frames in (b). Black lines represent the main migrations seen with the corresponding velocities in km.day −1 . The colorbar represents the event depth. (Fig. 6 from Duverger et al., 2018).

2.3 Long-term multiplet, seismicity rate, and the loading of major asperities

Contrary to short-lived multiplets, long-term and regular multiplets are located deeper (7–10 km), under the northern coast, within a layer less than 0.3 km thick (Fig. 2.2). They do not show any migration during swarm sequences, and occur at the border of nearly planar structures with low seismicity rate, which we interpret as major, locked asperities. The steady activation of these multiplets is explained by aseismic slip on the fault surface at the periphery of these large, locked asperities.

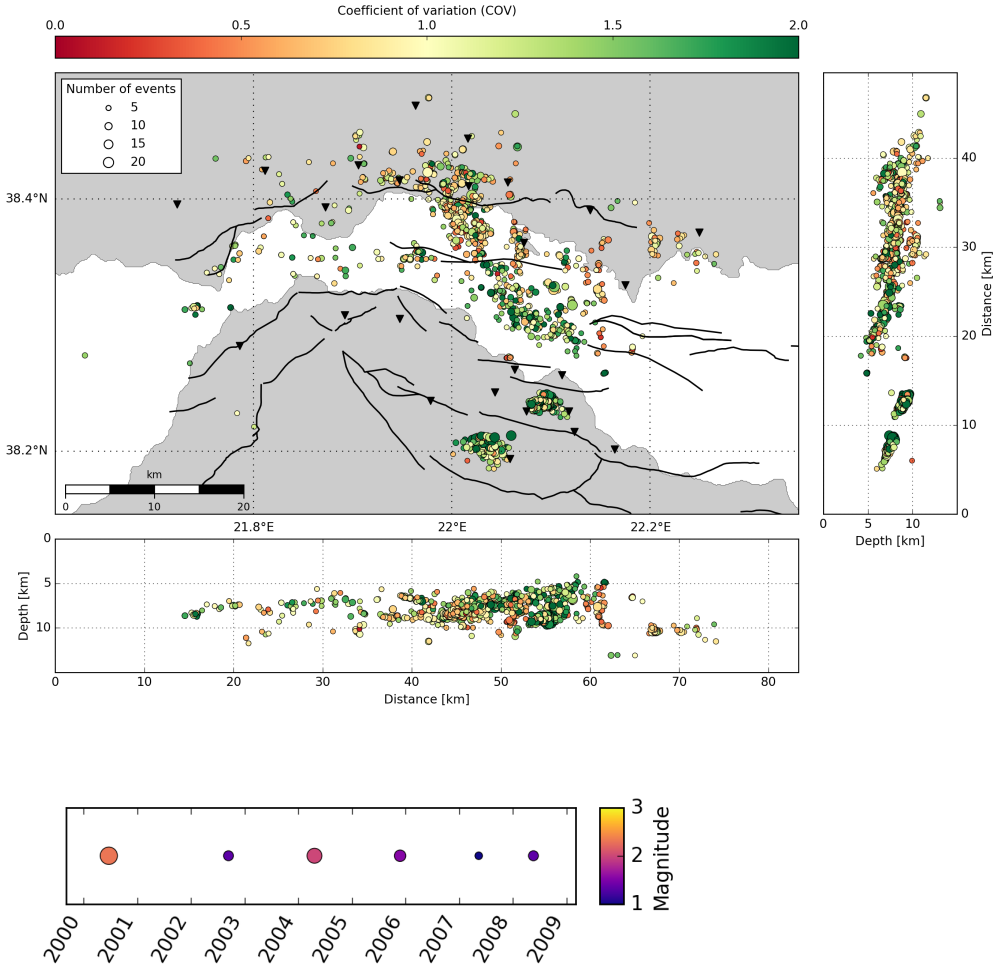

Figure 2.2 : Periodicity of repeaters. (top) Map cross-sections of repeaters having more than 5 events. Each circle represents a repeater, which is located at the mean hypocenter position of its relocated events. The circle size is proportional to the number of eventsin the repeater.The colors indicate the coefficient of variation (COV) of the inter-event times for each repeater. COV=0 for a fully periodic repeater. COV=1 for random inter-event times in the repeater. A larger COV corresponds to repeaters having some much longer and some much shorter inter-event times than its mean inter-event time. (bottom) Temporal occurrences of events for a quasi-periodic repeater. The color and the size of circles are proportional to the event magnitude.(from fig 11 of Duverger et al. ,2018)

Five major, possibly locked asperities are then identified on the main normal fault sytem (Fig. 2.3), using information from both the location of main regular multiplets, and the lower seismicity level.

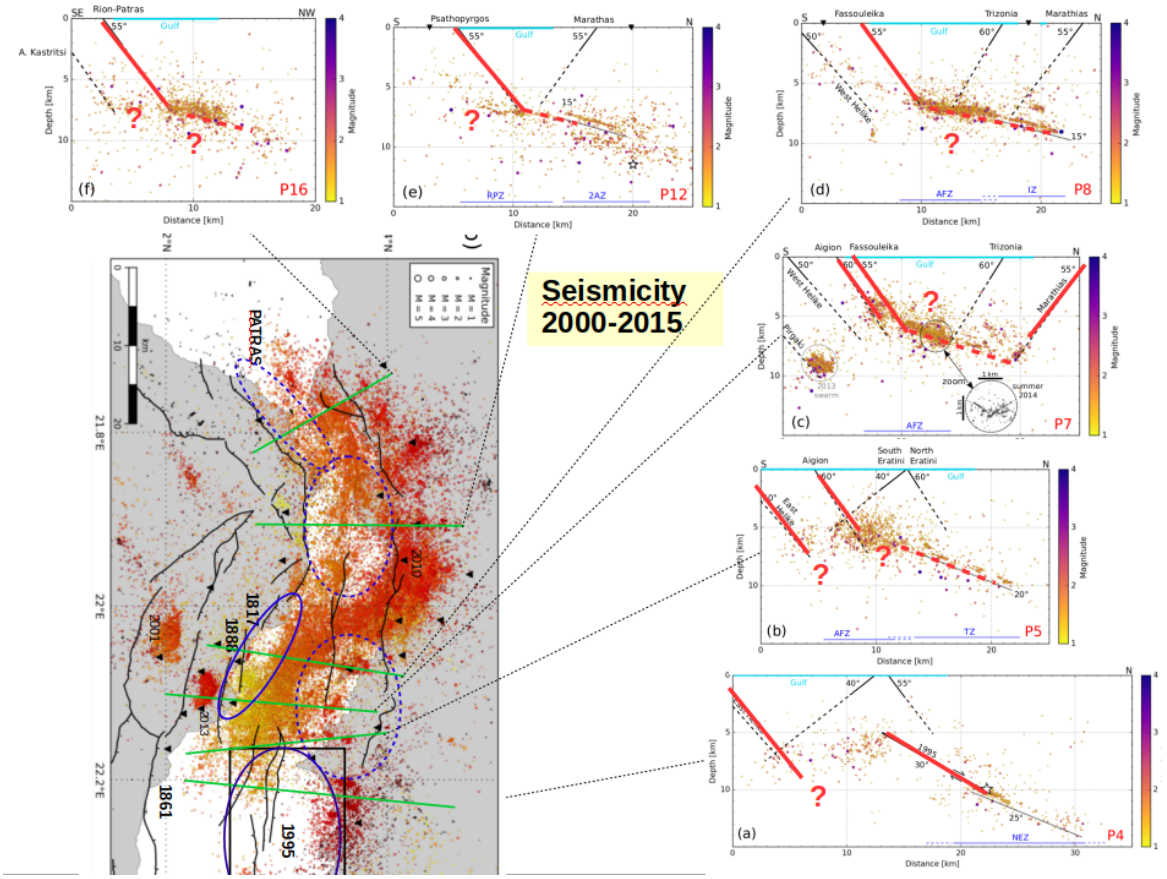

Fig. 2.3. Map and cross-sections of the microseismicity 2010-2015 in the western Rift of Corinth. Modified from Duverger et al. 2018. North is towards the right in the map. The red solid lines are the major normal faults. Dotted red lines are hypothetical fault segments. Blue ellipses are the major seismogenic asperities inferred from the space-time characteristics of the microseismicity.

- The eastern-most asperity (Section P4) provides the basis for our mechanical interpretation, as this asperity coincides with the main source area of the 1995 M6.3 rupture (Bernard et al., 1997) : it has a low level of seismicity rate, and is bounded west and north by long lasting multiplets.

- Moving west, two main asperities appear, at the longitude of the Aigion fault (P7-P8). The southern one is related to the Aigion fault itself, mostly locked from the surface to 6 km in depth, limited at depth by the highly fractured geological structure; the northern one is deeper, with a similar dip to that of the 1995 rupture. But contrary to the latter, which is a blind fault, it might be possible that during a dynamic rupture, this deeper asperity couples to the shallower Aigion fault into a single, large rupture, despite the heterogeneities and the expected shear release of the relay zone in-between both asperities. This could result in an M6.5 earthquake, instead of a M6 on either of the two asperities.

- Continuing westward, a zone of low seismicity (P12) characterizes the Psathopyrgos fault from the surface down to 10 km in depth. A dynamic rupture might thus be expected to propagate over the whole fault surface, with an M6+.

- Finally, the westernmost asperity is not so well resolved, due to the limit of the array, corresponding to the Rio-Patras fault system, crossing the Patras city.

References

References related to SERA

Aden-Antoniow, F., Étude des proprietés mécaniques et de la déformation transitoire dans les zones de subduction à partir de l'analyse de l'activité sismique, le cas du Chili., in French, PhD Thesis, Université de Paris, 2018.

Duverger, C. , S. Lambotte, P. Bernard, H. Lyon-Caen, A. Deschamps, A. Nercessian, Dynamics of microseismicity and its relationship with the active structures in the western Corinth Rift (Greece), *Geophys. J. Int.* 215, 196–221, https://doi.org/10.1093/gji/ggy264, 2018.

Other References:

Bernard, P., et al., The Ms=6.2, June 15, 1995 Aigion earthquake (Greece): evidence for low angle normal faulting in the Corinth rift, *Journal of Seismology 1,* 131-150, 1997.

Bouchon, M., Marsan, D., Durand, V., Campillo, M., Perfettini, H., Madariaga, R., & Gardonio, B. Potential slab deformation and plunge prior to the Tohoku, Iquique and Maule earthquakes, Nature Geoscience 9, 380–383 doi:10.1038/ngeo2701 (2016).

Herman, M. W., Furlong, K. P., Hayes, G. P., and Benz, H. M. (2016). Foreshock triggering of the 1 april 2014 mw 8.2 iquique, chile, earthquake. Earth and Planetary Science Letters, 447 :119–129.

Kato, A., Fukuda, J., Kumazawa, T., and Nakagawa, S. (2016). Accelerated nucleation of the 2014 iquique, chile mw 8.2 earthquake. Scientific reports, 6 :24792.

Katsumata, K. (2018). Long-term seismic quiescences and great earthquakes in and around the japan subduction zone between 1975 and 2012. In Earthquakes and Multi-hazards Around the Pacific Rim, Vol. I, pages 233–248. Springer.

Lambotte, S., H. Lyon-Caen, P. Bernard, A. Deschamps, G. Patau, A. Nercessian, F. Pacchiani, S. Bourouis, M. Drilleau, P. Adamova, Reassessment of the rifting process in the Western Corinth rift from relocated seismicity, *Geophys.J. Int.,*197,1822-1844, doi:10.1093/gji/ggu096, 2014.

Meng, L., Huang, H., Bürgmann, R., Ampuero, J. P., and Strader, A. (2015). Dual megathrust slip behaviors of the 2014 iquique earthquake sequence. Earth and Planetary Science Letters, 411 :177–187.

Métois, M., Vigny, C., and Socquet, A. (2016). Interseismic Coupling, Megathrust Earthquakes and Seismic Swarms Along the Chilean Subduction Zone (38°–18°S). Pure Appl.Geophys.DOI: 10.1007/s00024-016-1280-5 (2016).

Moreno, M., Haberland, C., Oncken, O., Rietbrock, A., Angiboust, S., and Heidbach, O. (2014). Locking of the chile subduction zone controlled by fluid pressure before the 2010 earthquake. Nature Geoscience, 7(4) :292.

Pasten-Araya, F., Salazar, P., Ruiz, S., Rivera, E., Potin, B., Maksymowicz, A., Torres, E., Villarroel, J., Cruz, E., Valenzuela, J., et al. (2018). Fluids along the plate interface influencing the frictional regime of the chilean subduction zone, northern chile. Geophysical Research Letters, 45(19) :10–378.

Poiata, N., C. Satriano, P. Bernard, and J.-P. Vilotte, Multiband backprojection method for detection and localization of seismic sources recorderd by dense seismic network, *Geophys. J. Int,* 205(3), 1548–1573, doi10.1093/gji/ggw071, 2016.

Poli, P., Jeria, A. M., and Ruiz, S. (2017). The mw 8.3 illapel earthquake (chile) : Preseismic and postseismic activity associated with hydrated slab structures. Geology, 45(3) :247–250.

Ruiz, S., Metois, M., Fuenzalida, A., Ruiz, J., Leyton, F., Grandin, R., Vigny, C., Goobar, A., Leibundgut, B., Annu. Rev. Nucl. Part. Sci. 61, Madariaga, R., Campos, J. Intense foreshocks and a slow slip

event preceded the 2014 Iquique M8.1 earthquake, Science , Vol. 345 no. 6201 pp. 1165-1169,DOI:10.1126/science.1256074 (2014).

Schurr, B. , et al., Gradual unlocking of plate boundary controlled initiation of the 2014 Iquique earthquake , Nature 512, 299–302 (2014).

Socquet, A., J.P. Vlades, J. Jara, F. Cotton, A. Walpersdorf, N. Cotte, S. Psetch, F. Ortega-Culaciati, D. Carrizo, and E. Norabuena, An 8 months slow slip event triggers progressive nucleation of the 2014 Chile megathrust (2017), Geophys. Res. Lett., 44, doi:10.1002/2017GL073023.

Wiemer, S. and Wyss, M. (1994). Seismic quiescence before the landers (M= 7.5) and big bear (M= 6.5) 1992 earthquakes. Bulletin of the Seismological Society of America, 84(3) :900–916.

Wu, Y.-M. and Chiao, L.-Y. (2006). Seismic quiescence before the 1999 chi-chi, Taiwan, Mw 7.6 earthquake. Bulletin of the Seismological Society of America, 96(1) :321–327.

Yoon, M., Buske, S., Shapiro, S., and Wigger, P. (2009). Reflection image spectroscopy across the andean subduction zone. Tectonophysics, 472(1-4) :51–61.

Zaliapin, I. and Ben-Zion, Y. (2013). Earthquake clusters in southern California I : Identification and stability. J. Geophys. Res. Solid Earth., vol. 118, 2847–2864, doi:10.1002/jgrb.50179, 2013.

Contact

Project lead	ETH Zürich
Project coordinator	Prof. Dr. Domenico Giardini
Project manager	Dr. Kauzar Saleh
Project office	ETH Department of Earth Sciences
	Sonneggstrasse 5, NO H62, CH-8092 Zürich
	sera_office@erdw.ethz.ch
	+41 44 632 9690
Project website	www.sera-eu.org